Eur. Phys. J. D (2012) 66: 328
DOI: 10.1140/epjd/e2012-30327-6

THE EUROPEAN PHYSICAL JOURNAL D

Regular Article

Nonlocal effects in the self-consistent nonlinear 3D propagation of an ultrastrong, femtosecond laser pulse in plasmas

D. Jovanović[1,a], R. Fedele[2,b], F. Tanjia[3,c], S. De Nicola[4,d], and L.A. Gizzi[5,e]

[1] Institute of Physics, University of Belgrade, P.O. Box 57, 11001 Belgrade, Serbia
[2] Dipartimento di Scienze Fisiche, Università di Napoli "Federico II" and INFN Sezione di Napoli, Complesso Universitario di M.S. Angelo, via Cintia, 80126 Napoli, Italy
[3] Scuola di Dottorato in Scienze Fisiche, Università di Napoli "Federico II" and INFN Sezione di Napoli, Complesso Universitario di M.S. Angelo, via Cintia, 80126 Napoli, Italy
[4] Istituto Nazionale di Ottica - CNR, Pozzuoli, Italy and INFN Sezione di Napoli, Complesso Universitario di M.S. Angelo, via Cintia, 80126 Napoli, Italy
[5] ILIL, Istituto Nazionale di Ottica - CNR, Pisa, Italy and INFN Sezione di Pisa, Pisa, Italy

Received 23 May 2012 / Received in final form 29 August 2012
Published online 27 December 20012 –

Abstract. A theoretical investigation of the interaction of an ultra-strong and ultra-short laser pulse with unmagnetized plasma is carried out and applied to the specifications of the Ti:Sa Frascati Laser for Acceleration and Multidisciplinary Experiments (FLAME). The analysis is based on the Lorentz-Maxwell fluid model in the fully relativistic regime taking the pancake approximation. The mathematical model yields Zakharov-like equations, which gives a satisfactory description of a wide range of laser-plasma acceleration configurations. It is shown that the pancake structure is unstable in two dimensions (2D) but the collapse occurs over a distance much longer than the typical active plasma length.

1 Introduction

The strong development of high-energy physics registered in the last two decades has required that particle accelerators have to work at the extreme conditions of luminosities and beam energy of the order of 10^{34} cm^{-2} s^{-1} and several tens of TeV or more, respectively. To satisfy these requirements, but keeping at the same time both the experimental set-up and the accelerating machine as compact as possible, very intense electromagnetic (e.m.) fields of about 100 GV/m are needed to manipulate the bunches of charged particles in appropriate ways (acceleration/deceleration, focusing/defocusing, wiggling, etc.). Unfortunately, the limitations in terms of costs and technologies, encountered in the use of the present generation of conventional accelerators, set the maximum acceleration gradient to a few tens of MeV/m. To overcome these limitations, the use of plasmas seems to be very promising to conceive new acceleration schemes and, in perspective, also the new, non-conventional, accelerating machines [1,2].

To produce e.m. fields in a plasma, charge separations and electric currents have to be excited by an external action. At the present time, on the basis of about 30 years of the research experience on the new acceleration techniques, the latter can be effectively provided by launching pulses of radiation [3–6] as well as charged-particle bunches [7–9] into the plasma.

Recently, the studies of the e.m. pulse propagation in plasmas have witnessed a rapid growth, in connection with the wealth of nonlinear effects investigated as well as with the number of experimental techniques and devices realized at the frontiers of nonlinear optics capable of ultra-high laser radiation intensities and ultra-short pulse durations. This is testified, in diverse applications, by the number of very spectacular nonlinear effects observed, as well as by the physical mechanisms used [10,11]. In some of the recently proposed plasma-based accelerator schemes, ultra-short and ultra-intense e.m. pulses are propagating in a plasma and exciting the ultra-intense plasma fields [so-called laser wake fields (LWF)] that are following the laser pulse at its group velocity. This scheme is usually referred to as *laser wake field accelerator* (LWFA), and it is expected to provide ultra-intense acceleration and strong focusing gradients [1,2] at relatively low cost compared to conventional accelerators. A good example are the experiments of femtosecond laser pulse propagation, in which the laser wake field has been excited by ultra-short laser

[a] e-mail: djovanov@ipb.ac.rs
[b] e-mail: renato.fedele@na.infn.it
[c] e-mail: tanjia@na.infn.it
[d] e-mail: sergio.denicola@ino.it
[e] e-mail: la.gizzi@ino.it

pulses to provide ultra-intense plasma electric fields for plasma-based particle accelerator schemes [12]. Valuable recent experimental results in this area have shown the absolute feasibility beyond 1 cm acceleration with the record energy exceeding 1 GeV [13–19].

In general, the interaction between the ultra-short, ultra-intense laser pulse and the surrounding plasma consists of the number of electromechanical actions, that depend on the pulse intensity. In turn, these actions affect the collective pulse dynamics which is nonlinear, as well. Consequently, the plasma and the pulses are strongly coupled. The electromechanical actions can be longitudinal (self-compression/expansion, self-modulation, bunch lengthening/shortening, etc.) or transverse (self-focusing/defocusing, beam widening, etc.), but they have a three dimensional (3D) character, in general. Usually, these effects provide the physical mechanisms that may enhance an initially small perturbation in the beam amplitude, leading to the large variety of instabilities, such as the modulational instability, the filamentation and the collapse (in the broadest sense, they belong to the family of *coherent instabilities*).

When the dispersion and the nonlinearity act so that they balance each other, very robust structures (the solitons) are formed. Their character is associated with a very high stability, since they do not change the shape and they behave like particles when they interact with other similar structures. Typically, solitons can propagate, without changing their shape, over macroscopic distances.

Another important aspect of the self-consistent nonlinear dynamics of the large amplitude waves in plasmas is the *nonlocality*. It is typically introduced by the slow time-scale response of the medium to a large amplitude wavepacket, leading to the sort of *memory effect*. The *spatial nonlocality* in the systems governed by the Zakharov equations leads to a nonlinear Schrödinger equation, whose nonlinear term differs from the standard cubic one, and is typically expressed as the functional of the wave intensity $I(\vec{r},t)$ in an integral form, viz.

$$U(\vec{r},t) = \frac{1}{2\pi}\int \mathcal{K}(|\vec{r}-\vec{r}\,'|)\; I(\vec{r}\,',t)\; d\vec{r}\,', \qquad (1)$$

where the *nonlocality function* $\mathcal{K}(|\vec{r}-\vec{r}\,'|)$ is a kernel that is provided by the adopted physical model of the self-interaction.

The effects of the nonlocality in the nonlinear term of the nonlinear Schrödinger equation, applied to different physical areas, have received recently a lot of attention in the literature [20–33]. The earlier works mostly dealt with the following three types of nonlocality. The first is usually referred to as *thermal nonlocality*, that describes the effect of plasma heating on the propagation of electromagnetic waves and also the orientational nonlinearity of nematic liquid crystals. In this case, $\mathcal{K}$ has the form of the modified Bessel function of the second kind K_0 and the slow response is governed by a diffusion-type equation which is valid for a typical spatial diffusion scale that is large compared to the operating wavelength [26,29]. The second type of nonlocality can be named as the *dipolar nonlocality*. It is encountered in the *dipolar Bose-Einstein condensate*, where the nonlocal character of the interatomic potential is due to a long-range interaction of dipoles. Here $\mathcal{K}(|\vec{r}-\vec{r}\,'|) = (1/2\pi)\int d\vec{k}\;[1-\sqrt{\pi}\,k\;\exp(k^2)\;\mathrm{erfc}(k_\perp)]\;\exp[i\vec{k}\cdot(\vec{r}-\vec{r}\,')]$. Such condensate has been realized recently in experiments with chromium atoms which exhibit a strong magnetic-dipole moment [34,35]. Finally, the most widely used model is the rather unphysical, but extremely instructive, the so-called *Gaussian nonlocality* [23,30], for which $\mathcal{K}(|\vec{r}-\vec{r}\,'|) = \exp(|\vec{r}-\vec{r}\,'|^2/2)$. In spite of the fact that there is no known physical system which can be described by the exact Gaussian response, this model has served as the phenomenological example of a nonlocal medium, enabling, thanks to its form, an analytical treatment of the ensuing wave dynamics.

For the above three types of nonlocality, analytical solutions were obtained in the regimes of strong and weak nonlocality, when the characteristic scale of the nonlocality function was taken to be either much longer than that of the function $\sqrt{I}$, i.e. $\nabla\log\mathcal{K} \gg \nabla\log\sqrt{I}$ or much shorter, viz. $\nabla\log\mathcal{K} \ll \nabla\log\sqrt{I}$. The integrals of the form equation (1) were evaluated using the partial integration, and with the accuracy to the first order. The stability analysis with an arbitrary nonlocality function was performed in reference [20] where it was shown that, in most cases, the arrest of the perpendicular collapse takes place. More detailed analyses were performed for Gaussian and thermal cases [29]. The existence of soliton-like solutions in the presence of a thermal nonlocality was shown analytically and various soliton solutions were found in the thermal case [30,31], in two dimensions (2D) and three dimensions (3D), in strong Gaussian limits [21–23], in the strong thermal limit (so-called *Davey-Stewartson regime*) [25], in the weakly nonlocal cases in nonlinear optics [27] and in the laser-plasma interaction [24].

Nonlocal effects have been theoretically investigated also in the nonlinear and collective dynamics of a charged-particle bunch in the conventional high-energy accelerators [33] within the context of the Thermal Wave Model [36–38]. The analysis included the resistive part of the beam coupling impedance that gave rise to both the acceleration and the deformation of the particle bunch. The weak resistive effects slightly change the initial shape of the given soliton profiles, but an uniform acceleration occurs due to the nonlocal term [33]. More intense resistive effects produce sensitive distortion as well as the uniform acceleration of the initial soliton pulse with the evident reduction of its amplitude. However, for a large resistive part, the deformation leads to the self-steepening and eventually to the wave-breaking. In fact, for a very large resistive part of the longitudinal coupling impedance, semi-infinite shock-like solutions have been predicted [33].

When the laser propagation in plasmas occurs under the extremely large amplitude conditions, the phenomenon of the saturation of the nonlinearity in the nonlocal response may take place [39]. An important consequence of the saturable nonlinearity is the stabilization of the background localized solution in two dimensional

(2D) problems, that is well known e.g. in the nonlinear optics. The soliton bistability phenomenon in media with saturable nonlinearities was found in reference [28].

In synthesis, the broad problem of the plasma acceleration involves two families of processes that are subordinated to each other. The first concerns the nonlinear modifications of the plasma induced by an e.m. pulse and the subsequent feedback of the plasma on the pulse itself. This pair of concomitant processes constitute the self-consistent interaction of the laser pulse during its propagation in the plasma, which may assume a nonlocal character. When the wave amplitudes become extremely large, the nonlinear and nonlocal response may lead to the nonlinearity saturation that, in turn, may work as a stabilizing factor for the localized structures. The subordinated family of processes is the manipulation of an electron bunch, suitably injected into the plasma (external injection) and subsequently accelerated by the ultra-intense plasma fields (laser wake fields) [40], or violently created by the laser ponderomotive action that accelerates directly the plasma electrons to a very high energy within a very short distance (self-injection) [41].

Recently, the progress of ultra-short and ultra-intense laser beam driven experiments has become even more remarkable, thanks to the development of: (i) high quality ultra short and ultra intense laser pulses that rapidly opened the possibility to produce electron bunches with the maximum energy gain up to several tens of GeV within a few tens of centimeters, by means of the self-injection mechanism, as demonstrated in the range of different self-injection experimental configurations [13–19] and planned for the FLAME laser facility [42–44]; (ii) high-quality short and intense electron bunches to be used very efficiently for the external-injection mechanisms [45,46].

In this paper, we develop a self-consistent theoretical model to investigate, both analytically and numerically, the three-dimensional character of the effects that are produced by the wake field excitation of ultra-short and ultra-intense e.m. radiation pulses and the concomitant nonlinear and nonlocal character of the plasma response. Since under the action of large radiation intensities ($\gtrsim 10^{17}$ W/cm^2), the quiver velocity corresponds to the relativistic or ultra-relativistic motion of the plasma electrons (note that for intensities $\gtrsim 10^{14}$ W/cm^2, the electron motion is already weakly relativistic), we adopt the Lorentz-Maxwell fluid model for the plasma in the general relativistic regime. The latter is self-consistently coupled with the set of equations governing the modification of the medium (plasma) on the time scale that is long compared to that of the carrier e.m. pulse. We demonstrate that the nonlinear and nonlocal effects come mostly from the interaction between the electromagnetic pump wave with a Langmuir wave, whose frequency is considerably lower than that of the electromagnetic (laser) pump. To this end and within a relatively simple model, we develop an analytical approach (used also for numerical evaluations) that may provide satisfactory physical interpretations for the purely numerical results obtained from the usual simulation codes. We use the standard assumption [3–6,47] that the evolution of the pulse is relatively slow in the reference frame that travels with the pulse, which greatly simplifies the hydrodynamic equations for the electrons. In particular, we show that, beyond the slowly-varying amplitude approximation, the above coupled equations are reduced to a non-trivial pair of Zakharov-like equations. These equations are governing the self-consistent 3D spatio-temporal nonlinear and nonlocal evolution of the four-potential and suitably take into account both the ultra-short longitudinal and transverse spatio-temporal variations of the laser pump amplitude while propagating through the plasma. Our analytical and numerical investigations are finalized to give new insights on the feasibility or limitations in the realization of an efficient plasma acceleration that has been already tested in preliminary experiments devoted to the diverse aspects of very high energy gain, very intense focusing and production of radiation of very small wavelengths. A great effort in this direction is ongoing also at INFN (Istituto Nazionale di Fisica Nucleare) within the project SPARC LAB (SL), devoted to the R&D of plasma-based new acceleration techniques. The INFN effort is based on the use of the FLAME (Frascati Laser for Acceleration and Multidisciplinary Experiments) laser which provides one of the most powerful femtosecond pulsed laser with 10 Hz repetition rate presently available with a maximum power of 220 TW and the maximum intensities exceeding 10^{21} W/cm^2.

In the next section, we formulate the main assumptions used to develop the appropriate mathematical model, such as the plasma and laser characteristics, the geometry of the propagation and the model adopted for the $plasma + laser$ system. In order to take into account different experimental conditions, we define three different intensity regimes that actually, for a given maximum laser power, depend on the transverse beam spot size, $L_\perp$. In particular, we follow the evolution of a laser pulse in the form of pancake, i.e. we take that the effective longitudinal pulse length, L_z, is much smaller than $L_\perp$ (i.e. $L_z \ll L_\perp$). In Section 3, we present the basic equations of our problem. Starting from our system of fluid equations (Lorentz-Maxwell system) we obtain the system of two coupled equations for the scalar and vector potentials. This is done by using the conservation law for the generalized linear momentum. This system of equations is closed with both the continuity and the motion equations for the electron fluid. In Section 4, we determine the leading part of the complete set of fluid equations in terms of a stationary one dimensional (1D) solution propagating with the speed of light. In the reference frame moving at the group velocity, this solution allows us to reduce our system of fluid equations in the pair of coupled nonlinear partial differential equations for the four-potential. They describe the spatio-temporal evolution of the modulated e.m. wave that is coupled with the Langmuir wave via the nonlinearities that arise from the relativistic effects. Such representation is valid for all the regimes of intensity and it plays the role that is more general than the one played by the Zakharov system of equations.

Subsequently, in Section 5, we introduce the modulational representation of the e.m. pulse, i.e. the vector potential is expressed as a vector amplitude modulating the carrier plane wave. The Zakharov-like system of equations, describing the spatio-temporal nonlinear and nonlocal evolution of the pancake-shaped laser pulse, is then obtained beyond the slowly-varying amplitude approximation and for arbitrary intensities. Provided that the form of the laser pulse is a pancake, such pair of equations is valid for all intensity regimes considered in this paper. In particular, the three different intensity regimes are further discussed and characterized in terms of the geometric beam features, such as the transverse space profile of the laser beam.

In Section 6, we consider the limiting cases of weak and moderate intensity regimes, that allow the power expansion in the nonlinear Poissons's equation. Such approximation yields a nonlinear Schrödinger equation with a reactive nonlocal nonlinear term, that is suitably discussed and numerically evaluated. The longitudinal nonlocal character of the pancake evolution is analyzed first and consecutively extended to study the 2D nonlinear and nonlocal evolution of the pulse. We show, in particular, the existence of the beam self-focusing and filamentation. We follow numerically the 2D evolution of the laser pulse for times that are comparable with the transit time of the pulse through the accelerator interaction chamber (∼10 cm) and study the interplay between the spreading and the collapse (filamentation) of the pulse in the transverse direction. We show that the pancake is unstable in 2D, but the collapse is not very fast. While the envelope of the laser pulse is not much affected by the collapse, relatively slow transverse contractions of the electrostatic potential are observed. In addition, the weak intensity pulses behave similarly to the standard NLS solitons and survive unchanged during a time much longer than that required for the laser accelerator scheme. So, within the present preliminary analysis, we do not expect that the transverse collapse constitutes a critical limitation for the self-injection accelerator scheme under investigation with FLAME. In Section 7 the pair of coupled equations given in Section 4 are specialized in the limiting case of very large intensities associated with the pancake evolution. Under these extreme conditions, the nonlinearity saturation is taken into account and used to reduce those pair of equations in the form of a Zakharov-like system of equations. In the course of such violent laser-plasma interaction, the channelling and the cavitation effects are expected to take place during the laser propagation. Conclusions and remarks are finally presented in Section 8.

2 Basic assumptions

Our basic assumptions of the laser are mainly formulated on the basis of the principal characteristics of the Ti:Sa laser FLAME [48]. In particular, the laser pulse carries the energy $E = 7$ J before compression, which for a compression efficiency of 70% gives a pulse energy of approximately 5 J. The minimum pulse duration is $\tau \geq 23$ fs and the maximum power is therefore $W_{max} \sim 220$ TW, at the wavelength $\lambda = 0.8$ μm, (which corresponds to $\omega = 2.36 \times 10^{15}\,\mathrm{s}^{-1}$), and repetition rate is $\nu_{rep} = 10$ Hz. It is worth noting that $\tau = 25 \times 10^{-15}$ s corresponds to the pulse length $L_z = 7.5$ μm, i.e. there are around 10 wavelengths of the laser light within the pulse. According to references [49,50], the plasma density in different experiments where FLAME is employed ranges as $n_e = (0.6 - 1) \times 10^{19}$ cm^{-3}, and even $4 \times 10^{19}\,\mathrm{cm}^{-3}$. The electron density $n_e = 10^{19}\,\mathrm{cm}^{-3}$ corresponds to the plasma frequency $\omega_{pe} = 1.78 \times 10^{14}$ s^{-1}. Thus, the pulse duration is roughly $\tau = 0.7\,T_p$, where T_p is the plasma period $T_p \equiv 2\pi/\omega_{pe} = 35.22 \times 10^{-15}$ s, while the collisionless skin depth (which is the wavelength of the natural oscillation mode of the plasma), $d_e \equiv 2\pi c/\omega_{pe} = 10.56$ μm is one order of magnitude longer than the laser wavelength ($\lambda = 0.8$ μm) and close to the pulse length ($L_z = 7.5$ μm).

Ranging from weak to strong laser intensities, we can take into account the diverse physical conditions of the pancake ($L_z \ll L_\perp$) propagation that correspond to different experimental conditions.

We take that the electric field of the laser light is sufficiently strong for the electrons to achieve relativistic jitter velocities. In particular, for the maximum laser power of the order of 220 TW, we consider three different regimes that are extrapolated from the various experiment proposals available in literature. Namely:

(i) *weak intensity regime* (WIR), where the maximum intensity I_{max} is roughly ranging from 2.5×10^{14} to 2.5×10^{16} W/cm^2 [51–53];
(ii) *moderate intensity regime* (MIR), where the maximum intensity I_{max} is roughly ranging from 1.5×10^{18} to 3×10^{19} W/cm^2 [53,54];
(iii) *strong intensity regime* (SIR), where the maximum intensity I_{max} is roughly ranging from 10^{20} to 2.5×10^{22} W/cm^2 [53,55]. This very high intensity regime will be accessible with FLAME only by means of the phase front correction, that is planned in the near future, and using very fast focusing optics in order to reach a 1 μm diameter focal spot.

Note that: for WIR, $L_\perp$ ranges roughly from 0.1 to 1 cm; for MIR, from 30 to 130 μm; for SIR, from 1 to 16 μm. However, in the physical conditions of SIR it turns out that $L_\perp$ and L_z (typically, ∼7.5 μm) would be of the same order of magnitudes, against the assumption of a pancake geometry. Actually, to reach the SIR within the same assumtion we have to assume that L_z be reduced to 1/3 of its typical value, i.e. $L_z \sim 2.5$ μm. This aspect will be deepened in Section 7, where the limit of strong intensities is discussed.

In the FLAME plasma-based accelerator scheme, the plasma is created in a helium gas jet by the laser ionization. A qualitative assessment of the ionization process can be obtained from the value of the Keldysh parameter $\Gamma = \sqrt{U_i/\mathcal{E}}$, where U_i is the ionization potential and $\mathcal{E}$ is the kinetic energy of the electron quiver motion in the laser field, $\mathcal{E} = \alpha^2 e^2 E_0^2/2\ m_e\ \omega^2$. Here $-e$ and m_e are the electron charge and mass, respectively, E_0 and ω are

the laser electric field amplitude and angular frequency, and $\alpha^2 = 1$ for a linear polarization, $\alpha^2 = 2$ for a circular polarization. For small values of the Keldysh parameter, $\Gamma \ll 1$, the optical field ionization leads to an almost instantaneous freeing of the electron and plasma formation, while in the opposite case $\Gamma \gg 1$, the multiphoton ionization dominates, see the review [56]. For helium, the potentials of the first and the second ionization are $U_{i1} = 24.5874$ eV and $U_{i2} = 54.416$ eV, respectively. Thus, the Keldysh parameter for a double ionization of He, in the MIR (moderate intensity regime) scales as $0.01/\alpha \lesssim \Gamma \lesssim 0.003/\alpha$ and in the WIR (weak intensity regime) as $0.1/\alpha \lesssim \Gamma \lesssim 1/\alpha$. For such large electric fields, as in the MIR, the ionization occurs instantaneously. This can be seen in the simple quasi-classical picture of the optical field ionization [56,57], when the laser field (regarded as quasi-static) is described by an electrostatic potential $-rE$ that is additive to the Coulomb potential of the nucleus. When the potential of the laser field is sufficiently strong, so that the total potential barrier lies below the electron energy level $-U_i$, the electron is free. The minimum laser intensity for which such barrier suppression ionization (BSI) occurs is easily calculated as

$$I_{BSI}\ [\mathrm{W/cm^2}] = 4.00 \times 10^9\, Z^{-2}\, U_i^4\ [\mathrm{eV}], \qquad (2)$$

where Z is the nucleus charge. For helium, the BSI threshold is found to be $I_{BSI} = 8.77 \times 10^{15}$ W/cm^2, which is three to four orders of magnitude smaller than the laser intensity in MIR, and comparable with that in WIR. However, a high level of ionization occurs also in WIR, since the quantum distribution function of the electron allows it to tunnel under the barrier and leave the atom even if the intensity is below the threshold. Terawatt-power laser systems of moderate size can have the electric field strength above 10^{10} V cm^{-1}. In such intense fields, the over-barrier ionization of atoms occurs in atomic time on the order of 10^{-17} s [58]. The experiments on propagation of a laser pulse of moderate relativistic intensity in He of density suitable for electron acceleration [59], confirmed also by simulations [60], have shown a rather stable propagation with weak refractive effects associated with the different degrees of ionization. In the focal region, ionization driven effects were limited to the lateral wings of the pulse. The precursors of the pulse were observed to pre-ionize the focal region, but they did not trigger propagation instabilities. As a result, an intermediate range of intensities was established, in which the ionization was too fast to perturb the propagating pulse, the relativistic effects were weak, and the ponderomotive effects appeared to be slow.

Finally, we assume that the above laser pump is travelling in an initially-homogeneous, unmagnetized plasma, where the ions are regarded as infinitely massive, forming therefore a background of positive uniform charge with number density n_0. Within the fluid theory, the system *plasma + laser* is described by the Lorentz-Maxwell system of equations in the fully relativistic regime. Given the above laser intensities, the radiation pressure (ponderomotive effect) is much greater than the kinetic pressure. Therefore, to the ends of the present investigation, the plasma can be regarded as a cold fluid [61].

3 Basic equations

According to Section 2, starting from the Lorentz-Maxwell system, it is the most convenient to write the wave equation, i.e. the equation for the electromagnetic field, expressing the electric and magnetic fields via the electrostatic potential ϕ and the vector potential $\vec{A}$, using the Coulomb gauge, $\nabla \cdot \vec{A} = 0$. Then, the Ampere's law

$$\nabla \times \vec{B} = \frac{1}{c^2}\left(\frac{\partial \vec{E}}{\partial t} + \frac{\vec{j}}{\epsilon_0}\right), \qquad (3)$$

(here $\vec{j}$ is the current density), is readily rewritten as

$$\frac{\partial^2 \vec{A}}{\partial t^2} - c^2 \nabla^2 \vec{A} + \nabla \frac{\partial \phi}{\partial t} = \frac{\vec{j}}{\epsilon_0}. \qquad (4)$$

For our purposes, it is more convenient to use only the component of equation (4) that is perpendicular to the direction of propagation of the laser beam (which is taken to be along the z-axis), and the divergence of equation (4) (i.e. the Poisson's equation), viz.

$$\frac{\partial^2 \vec{A}_\perp}{\partial t^2} - c^2\left(\nabla_\perp^2 + \frac{\partial^2}{\partial z^2}\right)\vec{A}_\perp + \nabla_\perp \frac{\partial \phi}{\partial t} = \frac{\vec{j}_\perp}{\epsilon_0}, \qquad (5)$$

$$\left(\nabla_\perp^2 + \frac{\partial^2}{\partial z^2}\right)\phi = -\frac{\rho}{\epsilon_0}, \qquad (6)$$

where ρ is the charge density that satisfies the continuity equation $\partial\rho/\partial t + \nabla \cdot \vec{j} = 0$. The current and the charge density are calculated as

$$\rho = \sum_\alpha q_\alpha n_\alpha, \quad \vec{j} = \sum_\alpha q_\alpha n_\alpha \vec{v}_\alpha, \qquad (7)$$

where q_α is the charge of the particle species α, and the hydrodynamic densities n_α and velocities $\vec{v}_\alpha$ are calculated from the appropriate hydrodynamic equations. For simplicity, we take that the characteristic frequency of the laser light and of the other processes involved is so high, compared to the plasma frequency, that the ions are essentially immobile. This justifies the assumption taken above of infinitely massive ions, constituting a neutralizing background for the electrons, i.e. $n_i = n_0$. In other words, we consider the interaction of high frequency electromagnetic and Langmuir waves, while the acoustic phenomena are disregarded. The electrons are regarded as cold, i.e. the phase velocity of the nonlinear modes involved are assumed to be much higher than the electron thermal velocity. The same regime is studied also in the standard literature, see e.g. references [3–6,47,62,63]. Then, the electron continuity and momentum equations take the form

$$\frac{\partial n}{\partial t} + \nabla \cdot (n\vec{v}) = 0, \qquad (8)$$

$$\left(\frac{\partial}{\partial t} + \vec{v} \cdot \nabla\right)\vec{p} = q\left[-\nabla\phi - \frac{\partial \vec{A}}{\partial t} + \vec{v} \times \left(\nabla \times \vec{A}\right)\right], \qquad (9)$$

where, for simplicity, the subscript for electrons has been omitted and $q = -e$. Here $\vec{p}$ is the electron momentum, which is related with the electron velocity $\vec{v}$ through the standard relativistic relation

$$\vec{v} = \frac{\vec{p}}{m_0\gamma}, \tag{10}$$

where m_0 is the electron rest mass, γ is the relativistic factor, $\gamma = (1 + p^2/m_0^2c^2)^{\frac{1}{2}}$, and c is the speed of light. Using the identities

$$(\vec{v}\cdot\nabla)\,\vec{p} = \vec{v}\times(\nabla\times\vec{p}) + (\nabla\vec{p})\cdot\vec{v} \text{ and } (\nabla\vec{p})\cdot\vec{v} = m_0c^2\nabla\gamma, \tag{11}$$

the electron momentum equation (9) is rewritten as

$$\frac{\partial}{\partial t}\left(\vec{p}+q\vec{A}\right) - \vec{v}\times\left[\nabla\times\left(\vec{p}+q\vec{A}\right)\right] + \nabla\left(m_0c^2\gamma + q\phi\right) = 0. \tag{12}$$

For later purposes, we write explicitly the transverse and the longitudinal components of equation (12), viz.

$$\left(\frac{\partial}{\partial t} + \vec{v}_\perp\cdot\nabla_\perp + v_z\frac{\partial}{\partial z}\right)\left(\vec{p}_\perp + q\vec{A}_\perp\right) - v_i\nabla_\perp\left(\vec{p}_i + q\vec{A}_i\right) + \nabla_\perp\left(m_0c^2\gamma + q\phi\right) = 0 \tag{13}$$

$$\left(\frac{\partial}{\partial t} + \vec{v}_\perp\cdot\nabla_\perp\right)(p_z + qA_z) - \vec{v}_\perp\frac{\partial}{\partial z}\left(\vec{p}_\perp + q\vec{A}_\perp\right) + \frac{\partial}{\partial z}\left(m_0c^2\gamma + q\phi\right) = 0. \tag{14}$$

4 Dimensionless equations in the moving frame

Following references [3–6,47,62,63] we consider the solution that is slowly varying in the reference frame that is moving with the velocity u in the direction of the z-axis. Using the dimensionless quantities

$$\vec{p}' = \frac{\vec{p}}{m_0c}, \quad \vec{v}' = \frac{\vec{v}}{c}, \quad \phi' = \frac{q\phi}{m_0c^2},$$
$$\vec{A}' = \frac{q\vec{A}}{m_0c}, \quad n' = \frac{n}{n_0}, \quad u' = \frac{u}{c},$$
$$t' = \omega_{pe}t, \quad \vec{r}\,' = \frac{\omega_{pe}}{c}\left(\vec{r} - \vec{e}_z\,ut\right), \tag{15}$$

where ω_{pe} is the plasma frequency of stationary electrons, $\omega_{pe} = (n_0q^2/m_0\epsilon_0)^{\frac{1}{2}}$, and making use of equation (7), we rewrite equations (5), (6), (8), (13), and (14) in the moving frame, viz.

$$\left[\frac{\partial^2}{\partial t^2} - 2u\frac{\partial^2}{\partial z\,\partial t} - \left(1-u^2\right)\frac{\partial^2}{\partial z^2} - \nabla_\perp^2\right]\vec{A}_\perp + \nabla_\perp\left(\frac{\partial}{\partial t} - u\frac{\partial}{\partial z}\right)\phi = \vec{v}_\perp n, \tag{16}$$

$$\left(\nabla_\perp^2 + \frac{\partial^2}{\partial z^2}\right)\phi = 1 - n, \tag{17}$$

$$\left(\frac{\partial}{\partial t} - u\frac{\partial}{\partial z}\right)n + \nabla\cdot(n\vec{v}) = 0, \tag{18}$$

$$\left(\frac{\partial}{\partial t} - u\frac{\partial}{\partial z} + \vec{v}_\perp\cdot\nabla_\perp\right)(p_z + A_z) - \vec{v}_\perp\frac{\partial}{\partial z}\left(\vec{p}_\perp + \vec{A}_\perp\right) + \frac{\partial}{\partial z}(\gamma+\phi) = 0, \tag{19}$$

$$\left[\frac{\partial}{\partial t} + (v_z - u)\frac{\partial}{\partial z} + \vec{v}_\perp\cdot\nabla_\perp\right]\left(\vec{p}_\perp + \vec{A}_\perp\right) - v_i\nabla_\perp(p_i + A_i) + \nabla_\perp(\gamma+\phi) = 0. \tag{20}$$

Usually, the solution of the hydrodynamic equations (18)–(20) is sought in the quasistatic regime, i.e. when the solution is slowly varying in the moving reference frame

$$\frac{\partial}{\partial t} \ll u\frac{\partial}{\partial z}. \tag{21}$$

The hydrodynamic equations (18)–(20) remain very complicated and in the classical works [3–6,47,63], they are further simplified by taking u to be very close to the speed of light

$$1 - u \ll 1, \tag{22}$$

and assuming an almost 1D (one dimensional) regime

$$\nabla_\perp \ll \frac{\partial}{\partial z}. \tag{23}$$

Two comments are in order.

First, in references [3–6] the equations are written in a reference frame moving with the speed of light ($u = 1$ in dimensionless units). However, with such a choice, an important dispersive term $\propto (1-u^2)\,\partial^2\vec{A}_\perp/\partial z^2$ is lost in the wave equation, which makes the further analysis and ordering more difficult. Following reference [47] we take u which is equal to the group velocity of an electromagnetic wave. For the FLAME laser frequency and plasma density, the latter is sufficiently close to the speed of light and one may apply the ordering (22).

Second, the 1D assumption (23) is valid for the perpendicular momentum equation (20) under the FLAME conditions and for all spot sizes. Conversely, it will be shown below that the quantities associated with the electrostatic components, viz. $\phi, n, \vec{v}_z, \vec{p}_z$, and $\vec{A}_z$, scale with the envelope of the laser pulse rather than with the electromagnetic wave. Thus, the 1D assumption (23) is appropriate for the continuity and the parallel momentum equations, equations (18) and (19), only when $L_z \ll L_\perp$ (i.e. in the pancake regime).

For a stationary 1D solution propagating with the speed of light, setting $\partial/\partial t = \nabla_\perp = 1 - u = 0$, the leading order parts of equations (18)–(20) are obtained in the

simple form

$$\frac{\partial}{\partial z}\left[\left(v_z-1\right)n\right]=0, \tag{24}$$

$$\frac{\partial}{\partial z}\left(-p_z+\gamma+\phi\right)=0, \tag{25}$$

$$\frac{\partial}{\partial z}\left(\vec{p}_\perp+\vec{A}_\perp\right)=0, \tag{26}$$

while from $\nabla\cdot\vec{A}=0$, within the same accuracy, we have

$$\frac{\partial A_z}{\partial z}=0. \tag{27}$$

Noting that for $z\to\pm\infty$ we have $\phi=\vec{A}=\vec{v}=\vec{p}=0$ and $\gamma=n=1$, and using $\gamma=(1+p_z^2+\vec{p}_\perp^{\,2})^{\frac{1}{2}}$, equations (24)–(27) are readily integrated, yielding

$$\left(v_z-1\right)n+1=0, \tag{28}$$

$$-p_z+\gamma-1+\phi=0, \tag{29}$$

$$\vec{p}_\perp+\vec{A}_\perp=0, \tag{30}$$

$$A_z=0. \tag{31}$$

Then, using the definition for γ and equations (28)–(30), after some straightforward algebra, we obtain the dimensionless charge and current densities as

$$n=\frac{\left(\phi-1\right)^2+\vec{A}_\perp^{\,2}+1}{2\left(\phi-1\right)^2}, \tag{32}$$

$$\vec{v}_\perp n=\frac{\vec{A}_\perp}{\phi-1}, \tag{33}$$

which permits us to rewrite our basic equations as

$$\left[\frac{\partial^2}{\partial t^2}-2u\,\frac{\partial^2}{\partial t\,\partial z}-\left(1-u^2\right)\frac{\partial^2}{\partial z^2}-\nabla_\perp^2+\frac{1}{1-\phi}\right]\vec{A}_\perp =-\left(\frac{\partial}{\partial t}-u\,\frac{\partial}{\partial z}\right)\nabla_\perp\phi, \tag{34}$$

$$\frac{\partial^2\phi}{\partial z^2}=\frac{\left(\phi-1\right)^2-1-\vec{A}_\perp^{\,2}}{2\left(\phi-1\right)^2}. \tag{35}$$

The above equations (34) and (35) constitute a system of coupled nonlinear equations that describe the spatio-temporal evolution of a modulated electromagnetic wave, in the form of a pancake, interacting with a Langmuir wave via the nonlocal nonlinearities that arise from the relativistic effects, beyond the slowly varying amplitude approximation and for an arbitrary intensity regime. They can not be simply regarded as the pair of Zakharov-like equations, but nevertheless they appropriately describe the parametric processes involved. Thus, besides the standard non-relativistic three-wave coupling phenomena (the Raman scattering), in the relativistic case, in principle, they may provide also the description of the four-wave processes, directly related to the modulational instability, soliton formation, etc. However, the actual nonlinear dynamics of the pulse strongly depends on the physical conditions in each particular device and can not be generalized. In Section 6, we apply equations (34) and (35) to WIR and MIR obtaining the suitable pair of Zakharov equations. They are used to describe the longitudinal 1D nonlocal response associated with the pulse dynamics that is then extended to the 2D nonlocal response. Equations (34) and (35) are then specialized to SIR of the pancake in Section 7.

We note that the nonlinear term in the wave equation (34), $\vec{A}_\perp/(1-\phi)$, tends to zero for very large Langmuir electrostatic potential. Thus, essentially different behavior is expected in the moderate and large intensity regimes, $\phi\ll 1$ and $\phi\gg 1$, respectively. Intuitively, we expect that this condition coincides with the similar condition for the laser intensity, $\vec{A}_\perp^{\,2}\ll 1$ and $\vec{A}_\perp^{\,2}\gg 1$. It will be shown below that with the present power of FLAME, in most experimental setups we have $\vec{A}_\perp^{\,2}<1$, and we can take the pulse to have a moderate intensity. Only in the case of strong focusing, the condition of large intensity ($\vec{A}_\perp^{\,2}\gg 1$) is satisfied, but such small spot size is not used in the accelerator scheme that is of our primary interest here. Furthermore, as we have already mentioned, in the latter case the longitudinal and transverse scales of the pulse are comparable, and the simple 1D approximation, equations (23)–(27) is not applicable.

5 Modulational representation and scalings

In the case of moderate intensities, we seek the solution of the wave equation in the moving frame (16) in the form of a modulated electromagnetic wave, viz.

$$\vec{A}_\perp=\vec{A}_{\perp_0}\,e^{-i\left[\omega' t-k'\left(z+ut\right)\right]}+c.c., \tag{36}$$

where the dimensionless frequency ω' and the dimensionless wavenumber k' are defined as

$$\omega'=\frac{\omega}{\omega_{pe}},\quad k'=\frac{ck}{\omega_{pe}}=\frac{d_e}{\lambda}, \tag{37}$$

where ω, k, and λ are the frequency, the wavenumber, and the wavelength of the electromagnetic laser wave, respectively. They satisfy the linear dispersion relation of electromagnetic waves, $\omega=\sqrt{c^2k^2+\omega_{pe}^2}$, whose dimensionless version has the form

$$\omega=\sqrt{k^2+1}. \tag{38}$$

For simplicity, hereafter, we drop the primes. We adopt u to be equal to the group velocity of the electromagnetic wave

$$u=\frac{d\omega}{dk}=\frac{k}{\omega}, \tag{39}$$

which permits us to rewrite the wave equation (16) and the Poisson's equation (17) as

$$2\,\mathrm{Re}\left\{e^{-i(t/\omega-kz)}\left[2i\,\omega\,\frac{\partial}{\partial t}-\omega^2\,\frac{\partial^2}{\partial t^2}+\left(k\,\frac{\partial}{\partial t}+\frac{1}{\omega}\,\frac{\partial}{\partial z}\right)^2+\nabla_\perp^2-\frac{\phi}{1-\phi}\right]\vec{A}_{\perp_0}\right\}=\left(\frac{\partial}{\partial t}-\frac{k}{\omega}\,\frac{\partial}{\partial z}\right)\nabla_\perp\phi, \tag{40}$$

$$\frac{\partial^2\phi}{\partial z^2}=\frac{(\phi-1)^2-1-\vec{A}_\perp^2}{2\,(\phi-1)^2}. \tag{41}$$

The pair of equations (40) and (41) can be regarded as a sort of generalized Zakharov system governing the envelope evolution of the laser for the pancake geometry beyond the slowly varying amplitude approximation.

Under the typical laser-plasma acceleration conditions under investigation with the FLAME laser as listed in Sections 1 and 2, the dimensionless frequency and wavenumber of the laser light are relatively large

$$\omega\approx k\gtrsim 12. \tag{42}$$

Likewise, the spatial derivative in the direction of propagation is estimated as

$$\frac{\partial\vec{A}_{\perp_0}}{\partial z}\sim\frac{\vec{A}_{\perp_0}}{L_z}, \tag{43}$$

where $L_z=\tau c=7.5\,\mu$m is the pulse length, whose dimensionless value, see equation (15), is $L_z'=\tau\omega_{pe}=4.46$. In the numerical simulations for MIR [49], a plasma density almost 50 times smaller plasma density was used ($n_e=1.5-2.5\times10^{17}$ cm^{-3}), which corresponds to $L_z'=0.7$ and $\omega'=100$.

With such small plasma density (i.e. with such large value of the parameter ω), the laser pulse tends to self-organize into a standard NLS (nonlinear Schrödinger) soliton with a linear phase, while the effects of a parabolic phase (often referred to as "the chirp") could be observed only for much larger laser intensities.

Requesting that, in the wave equation (40), the terms describing the temporal evolution of the envelope $\vec{A}_{\perp_0}$ and its spatial evolution in the direction of propagation are of the same order, we have (in dimensionless quantities (15))

$$\begin{aligned}\omega\,\frac{\partial\vec{A}_{\perp_0}}{\partial t}\sim\frac{1}{\omega^2}\frac{\partial^2\vec{A}_{\perp_0}}{\partial z^2}&\sim 4\times10^{-4}\,\vec{A}_{\perp_0}\\ &\gg\frac{k}{\omega}\,\frac{\partial^2\vec{A}_{\perp_0}}{\partial t\,\partial z}\sim 8\times10^{-6}\,\vec{A}_{\perp_0}\\ &\gg\omega^2\,\frac{\partial^2\vec{A}_{\perp_0}}{\partial t^2}\sim 16\times10^{-8}\,\vec{A}_{\perp_0}.\end{aligned} \tag{44}$$

Under these conditions, the 1D approximation in the hydrodynamic equations (18)–(20) is also justified. Likewise, from the first three terms in equation (44) we find that the envelope is slowly varying in time

$$\frac{\partial\vec{A}_{\perp_0}}{\partial t}\sim\frac{\vec{A}_{\perp_0}}{\omega^3L_z^2}\sim 2.42\times10^{-6}\,\omega\vec{A}_{\perp_0}\ll\omega\vec{A}_{\perp_0}. \tag{45}$$

The second derivative in time in equation (40) becomes relevant only in the case of a collapse, i.e. if the longitudinal size of the pulse becomes comparable to the laser wavelength, $\partial\vec{A}_{\perp_0}/\partial z\sim k\vec{A}_{\perp_0}$. We also note that, under the same conditions, the regimes of intensity defined in the Section 2 can be now expressed in terms of the following mathematical conditions:

(i) $\nabla_\perp^2\vec{A}_{\perp_0}\ll\left(1/\omega^2\right)\partial^2\vec{A}_{\perp_0}/\partial z^2$ corresponds to WIR;
(ii) $\nabla_\perp^2\vec{A}_{\perp_0}\sim\left(1/\omega^2\right)\partial^2\vec{A}_{\perp_0}/\partial z^2$ corresponds to MIR;
(iii) $\nabla_\perp^2\vec{A}_{\perp_0}\gg\left(1/\omega^2\right)\partial^2\vec{A}_{\perp_0}/\partial z^2$ corresponds to SIR.

However, for a fully 3D pulse, realized in the SIR, our equations (40) and (41) are applicable only if L_z is reduced in such a way to satisfy the pancake condition, i.e. $L_z\ll L_\perp$.

From the Poisson's equation (41) one can easily see that for a modulated electromagnetic wave (36), due to the presence of the term $\vec{A}_\perp^{\,2}$, the electrostatic potential contains a slowly varying component and a second harmonic, $\propto\exp[-2i(t/\omega-kz)]$. Thus, for a slowly varying amplitude (see condition (45)), the right-hand-side of the wave equation (40) is nonresonant and can be neglected, except in the case of a collapse, when both $\partial\vec{A}_{\perp_0}/\partial z\sim k\vec{A}_{\perp_0}$ and $\partial\vec{A}_{\perp_0}/\partial t\sim\omega\vec{A}_{\perp_0}$. However, in the case of a collapse it is not possible to use the 1D approximation (23) in the hydrodynamic equations (18)–(20), and the relatively simple model equations (40) and (41) are not applicable. For the same reason, we can neglect the second harmonic as nonresonant, also in the Poisson's equation (41). Particularly simple case is that of a circularly polarized wave

$$\vec{A}_\perp=A_{\perp_0}\,\frac{\vec{e}_x+i\vec{e}_y}{\sqrt{2}}\;e^{-i\left[\omega' t-k'(z+ut)\right]}+c.c., \tag{46}$$

when we have $\vec{A}_\perp^{\,2}=|A_{\perp_0}|^2$, i.e. the second harmonic is absent. Thus, in the absence of a collapse, our basic equation are simplified to

$$\left[2i\,\omega\,\frac{\partial}{\partial t}+\frac{1}{\omega^2}\frac{\partial^2}{\partial z^2}+\nabla_\perp^2-\frac{\phi}{1-\phi}\right]A_{\perp_0}=0, \tag{47}$$

$$\frac{\partial^2\phi}{\partial z^2}=\frac{(\phi-1)^2-1-|A_{\perp_0}|^2}{2\,(\phi-1)^2}, \tag{48}$$

where for a circularly and a linearly polarized wave we have $\vec{A}_{\perp_0}=(A_{\perp_0}/\sqrt{2})(\vec{e}_x+\vec{e}_y)$, and $\vec{A}_{\perp_0}=A_{\perp_0}\,\vec{e}_x$, respectively. Then, denoting by A_{max} the maximum amplitude of $A_{\perp_0}$, it is easy to see that, for circularly polarized waves, the maximum quiver velocity $\nu_{max}\equiv A_{max}/\sqrt{2}$ is given by

$$\nu_{max}=\frac{e}{m_0c^2\sqrt{2\pi^3\epsilon_0}}\,\frac{\sqrt{W_{max}}}{L_\perp}\sim\frac{6\times10^{-5}}{L_\perp}, \tag{49}$$

where $L_\perp$ is in meters. According to the definitions given in Section 2: $\nu_{max}\sim 6.3\times10^{-2}-6.3\times10^{-3}$ for WIR; $\nu_{max}\sim 2.1-0.5$ for MIR; $\nu_{max}\sim 63-4$ for SIR.

6 Weak and moderate laser intensities

For WIR and MIR, it is justified to assume (at least qualitatively) a small electrostatic potential, $\phi \ll 1$ (which in dimensional quantities corresponds to $\phi \ll m_0 c^2/e = 0.51 \times 10^6$ V), and expand the nonlinear terms in equations (47) and (48). Thus, for a weak and moderate intensity regimes, we have the following simplified equations

$$\left[2i\,\omega\,\frac{\partial}{\partial t} + \frac{1}{\omega^2}\frac{\partial^2}{\partial z^2} + \nabla_\perp^2 - \phi\right] A_{\perp_0} = 0, \tag{50}$$

$$\left(\frac{\partial^2}{\partial z^2} + 1\right)\phi = -\frac{|A_{\perp_0}|^2}{2}. \tag{51}$$

As the perturbation of the electron density, for the pancake structures, can be expressed from the Poisson's equation as $n - 1 = -\partial^2\phi/\partial z^2 \ll 1$, we note that, owing to such small density perturbation, both the WIR and MIR can be attributed as "linear regimes", defined in reference [51], p. 6 (see also figure 3 in Ref. [64]), in which our "quasistatic approximation" holds and a very detailed description of the nonlinear dynamics can be achieved within the applied semi-analytic model [1–6,47,62,63].

For the laser pulses that are much longer than the collisionless skin depth, d_e, one might set $\partial^2\phi/\partial z^2 \to 0$ in the Poisson's equation (48), which after the substitution in equation (50) gives rise to a standard cubic nonlinear Schrödinger equation. Such regime was studied extensively in reference [47]. However, under the plasma acceleration conditions under consideration here [48,59] listed in Section 1, the normalized pulse length, which is here defined as ratio between L_z and d_e, is ~ 1, and consequently $\partial^2\phi/\partial z^2 \sim \phi/L_z^2 \sim \phi$. This is particularly true for the *moderate intensity regime* [49]. Under such ordering, it is convenient to introduce the rescaled quantities $t \to \omega^3 t$, $\vec{r}_\perp \to \omega\vec{r}_\perp$, $\phi \to \phi/\omega^2$, and $A_{\perp_0} \to A_{\perp_0}/\omega$, when the above equations are rewritten as

$$\left(2i\,\frac{\partial}{\partial t} + \frac{\partial^2}{\partial z^2} + \nabla_\perp^2 - \phi\right) A_{\perp_0} = 0, \tag{52}$$

$$\left(\frac{\partial^2}{\partial z^2} + 1\right)\phi = -\frac{|A_{\perp_0}|^2}{2}. \tag{53}$$

The inhomogeneous linear equation (51) is easily solved in the form of a convolution, viz.

$$\phi(z,t) = \frac{\cos z}{2}\int_{z_1}^{z} dz'\,\sin z'\,|A_{\perp_0}(z',t)|^2 - \frac{\sin z}{2}\int_{z_2}^{z} dz'\,\cos z'\,|A_{\perp_0}(z',t)|^2, \tag{54}$$

where z_1 and z_2 are arbitrary initial positions.

First, we note that there exists a symmetric solution, which can be cast in the standard form of a *nonlocal response*, viz.

$$\phi(z,t) = \int d^3\vec{r}\,'\,R(|\vec{r} - \vec{r}\,'|)\,|A_{\perp_0}(\vec{r}\,',t)|^2, \tag{55}$$

where

$$R(|\vec{r} - \vec{r}\,'|) = -\frac{1}{4}\,\delta|x - x'|\;\delta|y - y'|\;\sin|z - z'|,$$

and the integration is performed for the entire space. It is interesting to note that, in the above, the nonlocality function R is not localized, in contrast to the standard examples of the nonlocal response, discussed in Section 1.

Obviously, the solution (55), that can be conveniently rewritten as

$$\phi(z,t) = -\frac{1}{4}\int dz'\,\sin|z - z'|\,|A_{\perp_0}(z',t)|^2, \tag{56}$$

is symmetric if $|A_{\perp_0}|$ is an even function of z, i.e. $|A_{\perp_0}(z,t)| = |A_{\perp_0}(-z,t)| \Rightarrow \phi(z,t) = \phi(-z,t)$.

6.1 1D longitudinal evolution of the pulse

It is worth noting that our equation (55) features the nonlocality only in the direction of propagation (i.e. in the direction of the z-axis), which is due to the effective 1D nature of the hydrodynamic equations in the regime when the perpendicular spot size is larger than the pulse length. Conversely, in the SIR, the hydrodynamic equations are much more difficult to solve and, apart from other complicacies, one may expect a full 3D nonlocal response of the pancake.

However, such nonlocality analyses are not relevant for our problem of propagation of a laser pulse in a nonlinear medium. Our problem is strongly asymmetric, i.e. virtually no response is expected to occur *in front* of the pulse. The solution (54) that is *driven by the laser pulse*, i.e. the one that is equal to zero in front of the pulse, has the form

$$\phi(z,t) = \frac{1}{2}\int_z^\infty dz'\,\sin(z - z')\,|A_{\perp_0}(z',t)|^2. \tag{57}$$

For a localized pulse in the vector potential, the solution (57) has the form of an oscillating wake. The amplitudes of the leading pulse-like structure and of the wake in the electrostatic potential, are determined by the width of the laser pulse. As a simple model, we have calculated the non-selfconsistent electrostatic response ϕ to Gaussian wavepackets, in the form $|A_{\perp_0}(z)|^2 = (1/2L)\,\exp(-z^2/2L^2)$, neglecting the feedback of the potential ϕ to the laser propagation. The solutions are displayed in Figure 1. We note that the electrostatic response (i.e. the form of the oscillating wake) strongly depends on the width of the laser pulse. If the width of the pulse is comparable to, or smaller than, the wavelength of the wake, $L \leq 1$, the wake is an almost purely sinusoidal function, existing only behind the laser pulse. If the laser pulse is somewhat larger than the wavelength, $L > 3.5$, the wake almost disappears and the electrostatic response is a single potential maximum that (almost) coincides with the envelope of the laser pulse. Already in the early paper [65] a nice study of the excitation of an oscillating tail was presented.

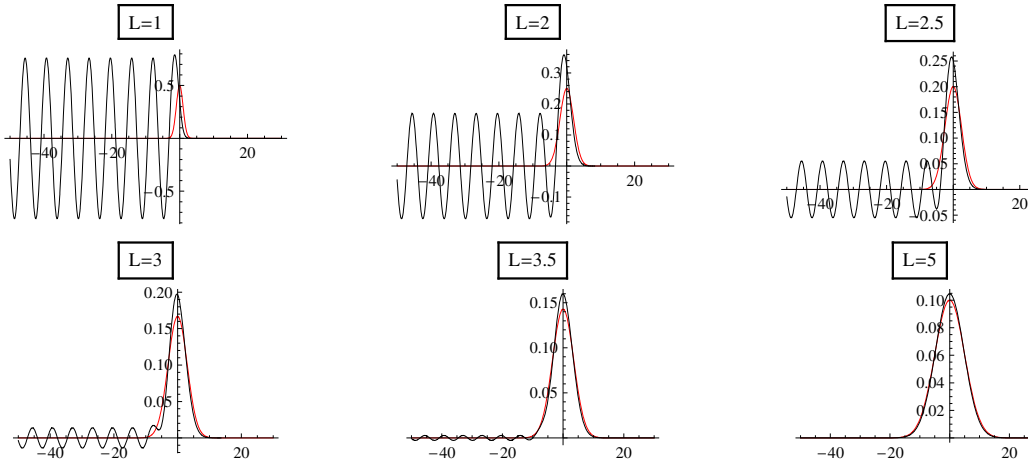

Fig. 1. (Color online) The electrostatic potential $-\phi$ (black line), found as the solution of equation (53) driven by a laser pulse with the Gaussian shape. The square amplitude of the vector potential (red line) is taken as $|A_{\perp_0}(z)|^2 = (1/2L)\ \exp(-z^2/2L^2)$, with different dimensionless pulse widths ranging from 1 to 5.

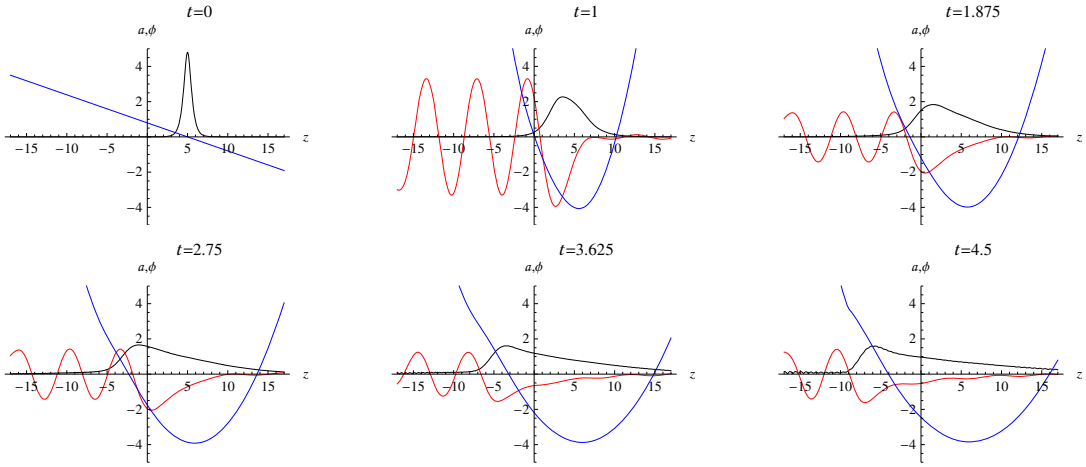

Fig. 2. (Color online) The evolution of a moderately focused laser pulse. The laser amplitude $a = |A_{\perp_0}|$ (black), the phase $\theta = \arg A_{\perp_0}$ (blue) and the electrostatic potential ϕ (red) are obtained as the numerical solutions of equations (52) and (53) in the 1D regime $\nabla_\perp \to 0$. The initial condition is solitonlike, i.e. $A_{\perp_0}(z,0) = 2\sqrt{C_1}\ \exp(i\,\delta k\,z)\ \mathrm{sech}\left(\sqrt{C_1}\,z\right)$, with $\delta k = -0.5$ and with a larger amplitude, $C_1 = 5.75$.

Obviously, in the strongly nonlinear regime when in equation (47) we have $\phi \sim 1$, the solution must be self-consistent. In other words, one must account for the feedback from the electrostatic wake (which is a spatially extended structure) to the electromagnetic pulse (which is localized in the direction of propagation). The conditions for the coexistence of such localized and extended components will be studied below.

The self-consistent nonlinear response in the *moderate intensity* regime and in the 1D limit was found by a numerical solution of equations (50) and (51), taking $\nabla_\perp = 0$. The results are displayed in Figure 2, in which we follow the temporal evolution of a pulse with the moderate intensity and with the initial solitonlike profile $A_{\perp_0}(z,0) = 2\sqrt{C_1}\ \exp(i\,\delta k\,z)\,\mathrm{sech}\left(\sqrt{C_1}\,z\right)$, with $C_1 = 5.5$. The observed behavior was considerably different than that of the *weak intensity* pulses. The amplitude very rapidly dropped to less than 1/2 of its initial value and continued to reduce, at a slower rate. Simultaneously, the pulse spread in the longitudinal direction and obtained a highly asymmetric shape – steep on the rear side and very gentle on the front side. The maximum of the pulse propagated backwards, as governed by our choice of a negative parameter $\delta k = -0.5$, but it was spreading so fast that its rear edge was actually moving forward. The phase of the laser amplitude, $\arg A_{\perp_0}$, was found to be an approximately quadratic function of z that did not propagate (in the moving frame) along z. Instead, it was spreading for larger times. Such behavior is typical for the *chirped solitons*. As the soliton velocity, in the case of linear phase, is proportional to the gradient of the phase, the observed spatial spreading of the chirped structures can be attributed to the change of sign of $d\theta/dz$ at $z \sim 6$.

In general, we may say that the solutions described here and in the preceding section are characterized by a chirp proportional to their peak power. Such chirp

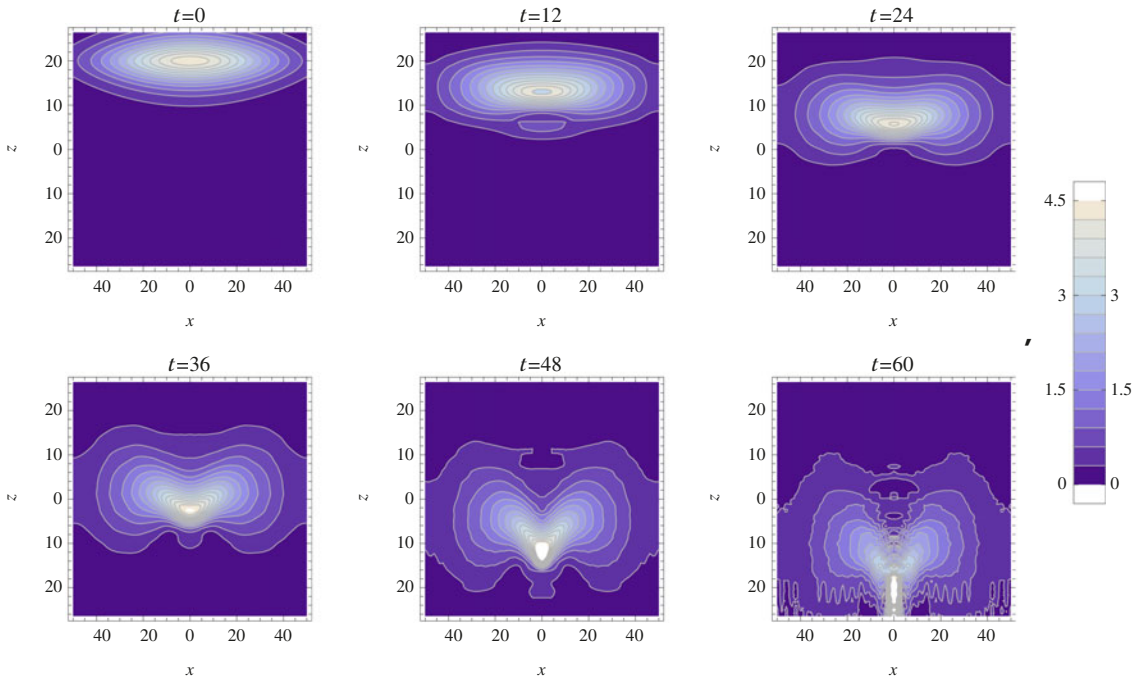

Fig. 3. (Color online) The evolution of the envelope of a weak intensity regime FLAME laser pulse, found as the numerical solution of equations (52) and (53) in the 2D regime $\nabla_\perp^2 = \partial^2/\partial x^2$. The initial condition was adopted in the form of an unchirped NLS soliton, that is modulated in the perpendicular direction by a Gausssian, $A_{\perp_0}(x,z,0) = 2\sqrt{C_1}\ \exp(-x^2/2L_x^2)\ \exp(i\,\delta k\,z)$ sech $(\sqrt{C_1}\,z)$, with $L_x = 25$, $C_1 = 0.07$, and $\delta k = -0.5$. The initial electrostatic potential was adopted to be zero, $\phi\,(x,z,0) = 0$.

dependence was observed earlier for the pulses in optical fibers near linear resonances [66].

6.2 Evolution of the pulse in two dimensions: self focusing

First, we have studied the 2D evolution of the coupled laser pulse/wakefield structure in the weak intensity regime, using the small-amplitude 1D solution as the initial condition. In the perpendicular direction, we artificially introduced a Gaussian shape of the pulse, whose characteristic spatial scale was adopted to be roughly $6-8$ time longer than the pulse length in the z-direction. For simplicity, we sought the solution in Cartesian coordinates, $\nabla_\perp^2 = \partial^2/\partial x^2$. These calculations were performed on a standard personal computer, using the numerical method of lines with 64×64 points. Such, relatively small, resolution was sufficient to reveal the main features of the 2D evolution and to follow the pulse for times longer than $t = 60$ in normalized units, during which the pulse travels approximately 17 cm in the laboratory frame. This is almost two times longer than the plasma length of 9.88 cm, quoted in reference [49]. The results are displayed in Figures 3 and 4. We found that a weak intensity structure is unstable in 2D, but the collapse is not very fast. We observed only a relatively slow transverse contraction for $t > 48$, which was different from what one expected intuitively. The simulations revealed that the velocity of propagation has the minimum in the centre. This is contrary to the expectation that a very strong laser pulse would push out all the electrons, so that the pulse, in the centre, propagate almost in a vacuum, by the speed of light. Instead, we have observed that the initial pancake folds, with the wings moving forward while the central part is falling back, obtaining a V-shape at the time $t \sim 24$. For very large times, the oscillating wake of the structure collapsed and disintegrated into a sequence of filaments in the z direction, whose longitudinal and transverse dimensions were of the same order and considerably smaller than the initial length of the pulse.

We studied also the 2D evolution in a moderate intensity regime, adopting the initial condition in the form of a unchirped NLS soliton with $C_1 = 5.5$, that is propagating backwards with $\delta k = -0.5$ (i.e. the same parameters as in the 1D case displayed in Fig. 2). We followed its evolution for a longer time than in the 1D case, until $t \gtrsim 15$. During this time, the pulse travels approx. 4.5 cm, which is about half the length of the interaction chamber. The results are displayed in Figures 5 and 6. The folding of the pancake-like pulse and the creation of a V-shape was observed after $t \sim 9$, which is considerably earlier than in the weak intensity regime. Virtually no perpendicular contraction was observed for $t \leq 15$, while the longitudinal stretching due to the negative chirp was similar to that observed in the 1D case. The related diminishment affected mostly the laser envelope, while the electrostatic potential still featured a sizable amplitude; the depth of its first minimum was more than 50% of its largest value, achieved shortly after the launch of the

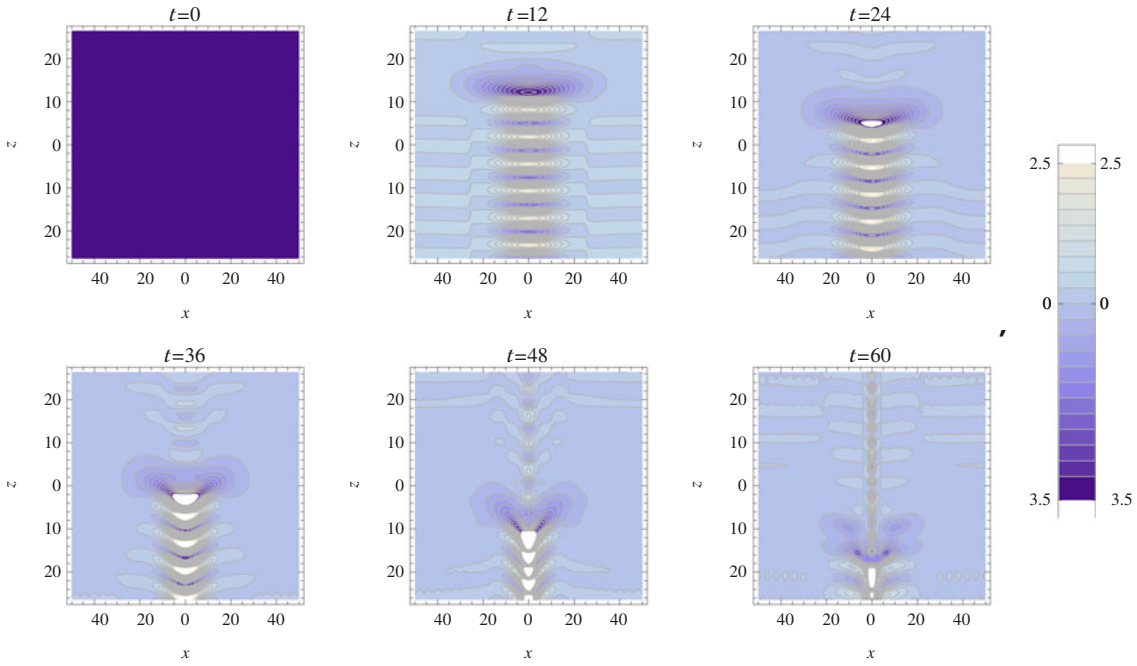

Fig. 4. (Color online) The evolution of the electrostatic potential produced by a weak intensity regime displayed in Figure 3.

pulse. The potential minimum obtained a V-shape in the x-z plane, but its cusp was somewhat broader than that of the weak intensity structures.

7 Regime of very large intensities

Here we want to outline some important aspects relevant for the near-future LWF-based experiments.

First of all, we observe that it is possible to reach the high intensity regime keeping satisfied the condition $L_z \ll L_\perp$, i.e. preserving the applicability of the pancake approximation (see Sect. 4). We expect that, in the near future, it might be technologically feasible to reduce the "pancake thickness" L_z to $\sim 1/3$ of its present value reached in high-power lasers. In the case of FLAME, this corresponds to the reduction of L_z from almost 10 μm to $2-3$ μm. Then, keeping the same maximum laser power W_{max} (for FLAME it is ∼220 TW), we may also focus the beam to ∼1/3 of the spot size that is presently used in the wakefield acceleration schemes with moderate laser intensities (for FLAME, this corresponds to the reduction of $L_\perp$ from 30 μm to 10 μm). In such a way, we reach the strong intensity regime with a pancake-shaped pulse (i.e. the pulse length is still much smaller than its width). Within such ordering of the laser power and pancake geometry, our equations (47) and (48) can be applied also in the *strong intensity* regime.

Another important aspect is related to the saturation of the nonlinearity in the nonlocal response and the subsequent stabilization of localized structures. We readily note that in the regime $|\phi| \gtrsim 1$ the nonlinear term is saturated. However, for such large amplitudes, using the representation of a modulated wave, equation (36), we find that the relative scaling of the terms on the left-hand-side of equation (40) is fundamentally different than in the case of moderate amplitudes. Obviously, the nonlinear term on the right-hand-side of equation (47) appears to be much larger than the linear terms, viz. $\phi/(1-\phi) \gtrsim 1 \gg \omega\,(\partial/\partial t) \sim (1/\omega^2)(\partial^2/\partial z^2)$. In other words, the ordering (44) that is the basic assumption used in the derivation of the model equation (40) breaks down in the large amplitude regime. An appropriate scaling is obtained if we take the velocity u to be equal to the speed of light, $u = 1$, and that the frequency and the wavenumber satisfy the dispersion relation of the electromagnetic waves in vacuum, $\omega = k$. Then, from equations (34) and (35), dropping the nonresonant (second harmonic) terms, we readily obtain:

$$\left[\frac{\partial}{\partial t}\left(2i\,\omega + \frac{\partial}{\partial t} - 2\,\frac{\partial}{\partial z}\right) + \nabla_\perp^2 - \frac{1}{1-\phi}\right] A_{\perp_0} \approx \left(2i\,\omega\,\frac{\partial}{\partial t} + \nabla_\perp^2 + \frac{1}{\phi}\right) A_{\perp_0} = 0, \quad (58)$$

$$\frac{\partial^2\phi}{\partial z^2} = \frac{(\phi-1)^2 - 1 - |A_{\perp_0}|^2}{2\,(\phi-1)^2} \approx \frac{\phi^2 - |A_{\perp_0}|^2}{2\phi^2}, \quad (59)$$

where we have expanded the nonlinear terms in the small quantity $1/\phi \ll 1$ and used the assumption of the weak modulation $\omega \gg \max(\partial/\partial t, \partial/\partial z)$.

We note from equation (58) that the regime of very large intensities is physically different from that of the moderate intensities. The wave equation (58) describes an electromagnetic wave propagating in vacuum, with a "small" nonlinear term $\propto 1/\phi$ added. This is due to the fact that the electron density perturbation, according to equation (32), is very large $\delta n = n - 1 = \mathcal{O}(1)$. This

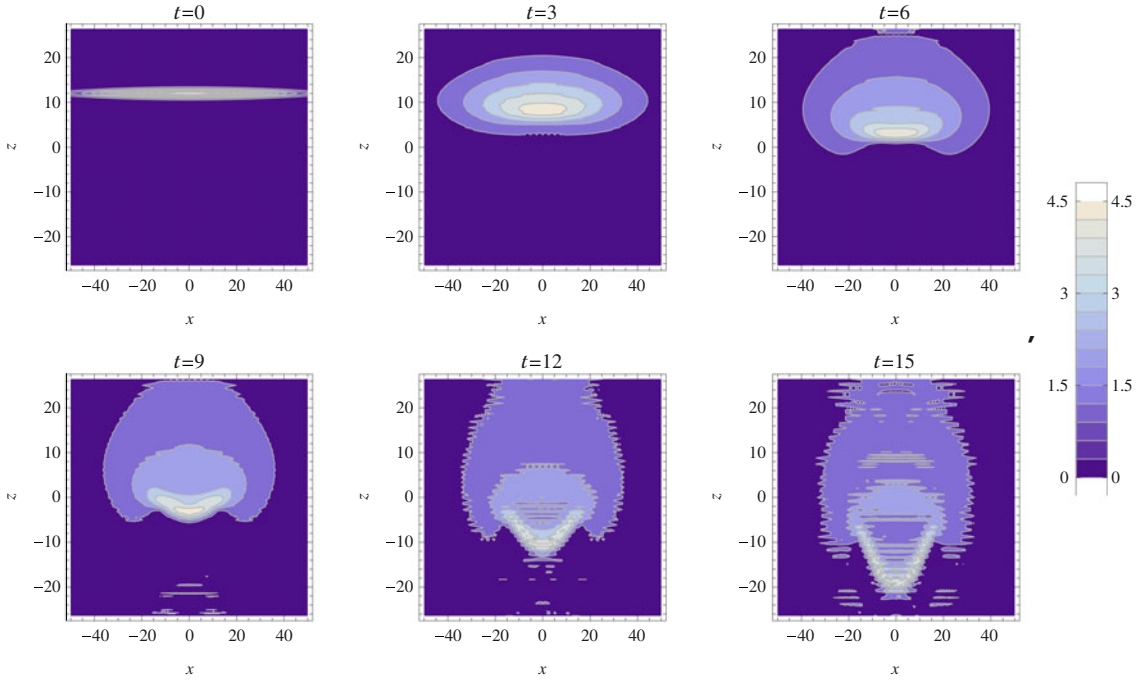

Fig. 5. (Color online) The evolution of the envelope of a laser pulse with the amplitude typical for the accelerator scheme under investigation here (referred to in the text as a moderate intensity regime). All parameters are the same as in Figure 3 except the amplitude, which is adopted as $C_1 = 5.5$.

corresponds to the creation of *vacuum channels* in the plasma, that is well known from numerical simulations. However, for a 2D or a full 3D picture in the large amplitude regime, one needs to use the general equation (40), since the intensity ϕ decreases radially, and close to the edges of the beam we are back to the $\phi \ll 1$ regime. Obviously, such task is numerically more demanding, and it will be considered separately, in a forthcoming publication. Furthermore, huge electric fields arising from such electron density perturbation, may affect also the ions, whose dynamics also needs to be taken into account.

8 Conclusions and remarks

In this paper, we have theoretically studied the self-consistent interaction between an ultra-strong, ultra-short laser pulse in the form of a pancake ($L_z \ll L_\perp$) and an unmagnetized plasma with the ions taken to be immobile. Within the framework of the laser wake field excitation, our study has been mainly referred, as a concrete example, to the FLAME laser which is currently employed as a facility in the Frascati National Laboratories of INFN for different plasma-based acceleration projects including the self-injection case. For the maximum laser power $W_{max} \sim 220$ TW, we have considered three different regimes of the laser intensities, corresponding to different transverse spot sizes of the pancake, respectively. Since in our physical problem the laser intensity ranges from 10^{14} to 10^{20} W/cm^2, the motion of the plasma electrons has been assumed to be in the fully relativistic regime. In addition, due also to the concomitant role of the high intensity and the high gradient of the laser field profiles, the radiation pressure effects (ponderomotive force) fairly overcome those arising from the electron kinetic pressure, so that the plasma can be regarded as being cold. We have adopted a fluid plasma model, described by the relativistic Lorentz-Maxwell equations, from which we have derived and solved numerically the nonlinear equations that describe a plasma penetrated by an ultrashort, ultrastrong laser pulse, in the fully relativistic regime. We used the numerical method of lines and the calculations were performed on a standard PC. To derive those equations, we have first determined the leading order part of our set of fluid equations in terms of a stationary 1D solution propagating with the speed of light. We have showed that, in the reference frame that is moving at the group velocity of the laser light, this solution have allowed us to reduce our system of fluid equations in a pair of coupled nonlinear partial differential equations for the four-potential. They describe the spatio-temporal evolution of the modulated e.m. wave that is coupled with the Langmuir wave via the nonlinearities arising from the relativistic effects. A Zakharov-like system of equations has been obtained beyond the slowly-varying amplitude approximation. It consists of a parabolic wave equation governing the nonlinear *high-frequency* propagation of $A_{\perp_0}$ that is coupled with the *slow* plasma response equation through the electric potential variation that, in turn, is driven by $A_{\perp_0}$. In the weak and moderate intensity regimes, a nonlinear Schrödinger equation with a reactive nonlocal nonlinear term has been obtained and numerically studied in both 1D and 2D cases. The evolution of the pancake has been followed for times that are comparable with the

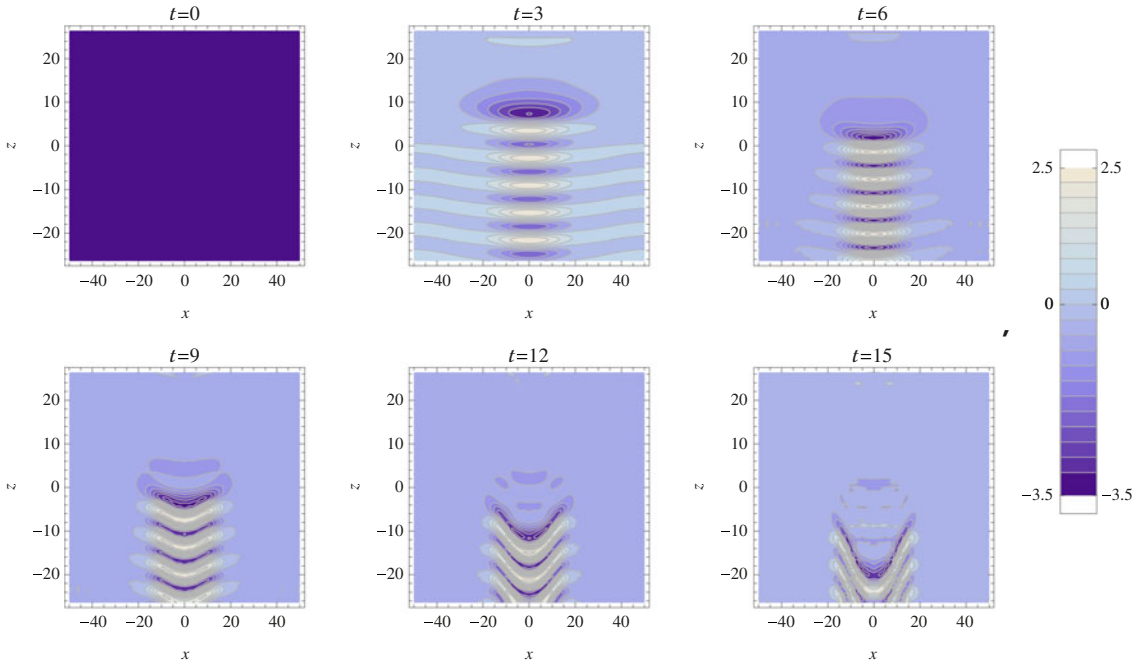

Fig. 6. (Color online) The evolution of the electrostatic potential produced by a moderate intensity regime displayed in Figure 5.

transit time of the pulse through the accelerators interaction chamber (∼10 cm) and studied the interplay between the spreading and the collapse (filamentation) of the pulse in the transverse direction, in spite of the numerical limitations imposed by the maximum resolution of 64 × 64 points, that we have used. We have shown that the 2D evolution of a pancake in the weak and moderate intensity regimes is unstable, but the collapse is not very fast. We have followed the evolution until the times during which the pulse travels (in the laboratory frame) the distance of about 17 cm, which is almost two times longer than the actual size of the interaction chamber in the laser accelerator device. While the envelope of the laser pulse was not much affected by the collapse, a relatively slow transverse contraction of the electrostatic potential was observed. In addition, we would like to emphasize that pulses whose intensities fall in the weak or moderate intensity ranges behave similarly to the standard NLS solitons and survive unchanged during a time sufficiently longer than required for the laser accelerator scheme. Thus, within this preliminary analysis, we do not expect that the transverse collapse constitutes a critical limitation for the accelerator scheme under consideration here.

In the strong intensity regime, we have outlined the role of the saturation of the nonlinear and nonlocal plasma response relevant to the pancake self-consistent evolution. For the typical maximum power and suitable choice of the longitudinal and the transverse dimensions of FLAME that preserve the 1D hydrodynamical approximation (see Sect. 4), we have found the appropriate set of Zakharov equations governing the pancake evolution that we have compared to the corresponding set of equation valid for the weak and moderate intensity regimes.

Remarkably, our approach provides a physical model in terms of the pair of coupled nonlinear partial differential equations (Zakharov-like system), widely used in plasma physics and in many other areas of nonlinear physics, that give suitable and appropriate descriptions of the laser-plasma interaction in the diverse regimes considered in this paper. Their analytical and numerical solutions (the latter have been obtained by a standard PC) may be very helpful and relevant to the interpretation of the results given by the standard simulation codes presently widely employed to describe the very violent self-consistent laser-plasma interactions.

Finally, we want to outline that a special care must be taken when the longitudinal nonlocality, as described by the pair of equations (47) and (48), is considered under the assumption such that $\phi \sim 1$. In fact, for consistency, one must account for the feedback from the electrostatic wake (which is a spatially extended structure) to the electromagnetic pulse (which is localized in the direction of propagation). The conditions for the coexistence of such localized and extended components will be studied in a forthcoming work.

Preliminary results [67] indicate an agreement between our semi-analytic results with those obtained using massive fluid simulations by the Pisa group in the moderate intensity regime. This work in progress will include also the considerations of the strong intensity regime, in the case of pancake pulses with slightly shorter lengths and smaller spot sizes, yielding an expulsion of electrons and the creation of vacuum channels.

Although the classical works [1–6,47,62,63] regard the relativistic plasma in a moderate intensity regime as a cold fluid [61], it is worth noting that the nonlinear contribution to the off-diagonal terms in the electron stress tensor may give rise to the non-curlfree component of the time-dependent ponderomotive force [68], that is one among the known mechanisms for the generation of quasi-stationary,

mega-Gauss magnetic fields[1]. Alternatively, it is usually thought [58] that the creation of a quasistationary magnetic field by a laser pulse with a duration < 0.1 ps, in a homogeneous, collisionless, and tenuous plasma, is likely to come from the jets of fast electrons arising in laser plasma. These jets are subject to the Weibel instability, leading to the current filamentation and the generation of a magnetic field [69,70]. As the latter is located mostly in the plasma wake, behind the main pulse [58,69], it is not expected to affect significantly the propagation of the laser pulse. For the spatial structure of such wake magnetic field see e.g. [71] and references therein. The magnetic field has been known to have a focusing effect on relativistic electrons in the plasma wakefield accelerator context [72]. The experimental results definitely indicate that the lifetimes of magnetic fields are considerably longer (by orders of magnitude) than the laser pulse duration [58]. The role of the self-generated magnetic field is beyond the scope of the present paper, and it will be the subject of a future study.

This work was supported in part by the grant # 171006 of the Serbian Ministry of Science and Education. One of the authors (DJ) acknowledges financial support from the fondo FAI of the Italian INFN and the kind hospitality of Dipartimento di Scienze Fisiche, Università di Napoli "Federico II". The authors also wish to thank Prof. Danilo Giulietti and Dr. Paolo Tomassini for enlightening discussions.

References

1. E. Esarey, P. Sprangle, J. Krall, A. Ting, IEEE Trans. Plasma Sci. **24**, 253 (1996)
2. R. Bingham, J.T. Mendonça, P.K. Shukla, Plasma Phys. Control. Fusion **46**, R1 (2004)
3. M.N. Rosenbluth, C.S. Liu, Phys. Rev. Lett. **29**, 701 (1972)
4. T. Tajima, J.M. Dawson, Phys. Rev. Lett. **43**, 267 (1979)
5. L.M. Gorbunov, V.I. Kirsanov, Zh. Eksp. Teor. Fiz. **93**, 509 (1987)
6. P. Sprangle, E. Esarey, A. Ting, G. Joyce, Appl. Phys. Lett. **53**, 2146 (1988)
7. P. Chen, Part. Accel. **20**, 171 (1986)
8. P. Chen, J.M. Dawson, R.W. Huff, T. Katsouleas, Phys. Rev. Lett. **54**, 693 (1985)
9. J.B. Rosenzweig, D.B. Cline, B. Cole, H. Figueroa, W. Gai, R. Konecny, J. Norem, P. Schoessow, J. Simpson, Phys. Rev. Lett. **61**, 98 (1988)
10. J.-C. Diels, W. Rudolph, *Ultrashort Laser Pulse Phenomena Fundamentals, Techniques, and Applications an a Femtosecond Time scale* (Elsevier, Amsterdam, 2006)
11. S.L. Chin, *Femtosecond Laser Filamentation* (Springer, Berlin, 2009)
12. F. Dorchies et al., Phys. Plasmas **6**, 2903 (1999)
13. J. Faure et al., Nature **431**, 541 (2004)
14. C.G.R. Geddes et al., Nature **431**, 538 (2004)
15. S.P.D. Mangles et al., Nature **431**, 535 (2004)
16. J. Faure et al., Nature **444**, 737 (2006)
17. W. Leemans et al., Nat. Phys. **2**, 696 (2006)
18. C.E. Clayton et al., Phys. Rev. Lett. **105**, 105003 (2010)
19. K.A. Marsh et al., Laser wakefield acceleration beyond 1 GeV using ionization induced injection, LLNL-PROC-476791 (2011) (also in Proc. Particle Accelerator Conference, New York, NY, USA, TUOBN1 (2011))
20. O. Bang, W. Królikowski, J. Wyller, J.J. Rasmussen, Phys. Rev. E **66**, 046619 (2002)
21. M.R. Belić, W.-P. Zhong, Eur. Phys. J. D **53**, 97 (2009)
22. W.-P. Zhong, L. Yi, R.-H. Xie, M. Belić, G. Chen, J. Phys. B **41**, 025402 (2008)
23. D. Briedis, D.E. Petersen, D. Edmundson, W. Krolikowski, O. Bang, Opt. Express **13**, 435 (2005)
24. L. Hadžievski, M.M. Škorić, M.S. Jovanović, L. Nikolić, in *Science of Superstrong Field Interactions*, edited by K. Nakajima and M. Deguchi, volume 634 of AIP Conf. Ser. (2002), p. 99
25. I. Kaminer, C. Rotschild, O. Manela, M. Segev, Opt. Lett. **32**, 3209 (2007)
26. I.A. Kol'Chugina, V.A. Mironov, A.M. Sergeev, JETP Lett. **31**, 304 (1980)
27. W. Królikowski, O. Bang, Phys. Rev. E **63**, 016610 (2001)
28. W. Królikowski, B. Luther-Davies, Opt. Lett. **17**, 1414 (1992)
29. Y. Lin, R.-K. Lee, Y.S. Kivshar, J. Opt. Soc. Am. B **25**, 576 (2008)
30. D. Mihalache, Rom. Rep. Phys. **59**, 515 (2007)
31. D. Mihalache, D. Mazilu, F. Lederer, B.A. Malomed, Y.V. Kartashov, L.-C. Crasovan, L. Torner, Phys. Rev. E **73**, 025601 (2006)
32. S. Skupin, O. Bang, D. Edmundson, W. Królikowski, Phys. Rev. E **73**, 066603 (2006)
33. P. Johannisson, D. Anderson, M. Lisak, M. Marklund, R. Fedele, A. Kim, Phys. Rev. E **69**, 066501 (2004)
34. S. Ronen, D.C.E. Bortolotti, D. Blume, J.L. Bohn, Phys. Rev. A **74**, 033611 (2006)
35. D.C.E. Bortolotti, S. Ronen, J.L. Bohn, D. Blume, Phys. Rev. Lett. **97**, 160402 (2006)
36. R. Fedele, G. Milele, Nuovo Cimento D **13**, 1527 (1991)
37. R. Fedele, G. Miele, L. Palumbo, V.G. Vaccaro, Phys. Lett. A **179**, 407 (1993)
38. D. Anderson, R. Fedele, V. Vaccaro, M. Lisak, A. Berntson, S. Johanson, Phys. Lett. A **258**, 244 (1999)
39. D. Suter, T. Blasberg, Phys. Rev. **48**, 4583 (1993)
40. A.G. Khachatryan, M.J.H. Luttikhof, A. Irman, F.A. van Goor, J.W.J. Verschuur, H.M.J. Bastiaens, K.-J. Boller, Nucl. Instr. Methods Phys. Res. A **566**, 244 (2006)
41. S. Kalmykov, S.A. Yi, V. Khudik, G. Shvets, Phys. Rev. Lett. **103**, 135004 (2009)
42. L. Labate et al., Radiat. Eff. Def. Solids **165**, 787 (2010)
43. L.A. Gizzi et al., Nuovo Cim. **32C**, 433 (2009)
44. S.M. Wiggins et al., Plasma Phys. Control. Fusion **52**, 124032 (2010)
45. V. Malka, A. Lifschitz, J. Faure, Y. Glinec, AIP Conf. Proc. **877**, 64 (2006)
46. W. Lu et al., Phys. Rev. Special Topics: Acc. Beams **10**, 061301 (2007)
47. V.I. Berezhiani, S.M. Mahajan, Phys. Rev. Lett. **73**, 1837 (1994)
48. G. Turchetti et al., *Optical acceleration activity in Italy: Plasmonx, Prometheus project* (2010), http://wwwapr.kansai.jaea.go.jp/pmrc_en/org/colloquium/download/colloquium16-1.pdf

[1] The kinetic description of the same mechanism was developed several decades ago, see [73] and references therein.

49. C. Benedetti et al., *NTA PLASMONX* (2008), http://www.lnf.infn.it/rapatt/2008/06/PLASMONX.pdf
50. L.A. Gizzi et al., Eur. Phys. J. Special Topics **175**, 3 (2009)
51. D. Giulietti et al., *Plasma acceleration and monochromatic X-ray production*, http://pcfasci.fisica.unimi.it/Pagine/Documenti/CDR_PLASMONX.pdf
52. C. de Martinis et al., *Proc. EPAC'06, Edinburgh, Scotland* (2006)
53. A. Giulietti et al., Phys. Plasmas **13**, 093103 (2006)
54. F. Broggi, L. Serafini, *Energy deposition effects of the X photon beam on the mirror of PLASMON-X experiment at* LI^2FE, INFN report SPARC-EBD-10/01 (2010), http://www.lnf.infn.it/acceleratori/sparc/TECHNOTES/EBD/SPARC_EBD_10_001.pdf
55. C. Benedetti et al., *NTA PLASMONX* (2008), http://www.lnf.infn.it/rapatt/2008/06/PLASMONX.pdf
56. A. Pukhov, Rep. Prog. Phys. **66**, 47 (2003)
57. S. Augst, D.D. Meyerhofer, D. Strickland, S.L. Chin, J. Opt. Soc. Am. B **8**, 858 (1991)
58. V.S. Belyaev, V.P. Krainov, V.S. Lisitsa, A.P. Matafonov, Phys. Usp. **51**, 793 (2008)
59. A. Giulietti, *Seminario PlasmonX Risultati dell'esperimento ILIL/SLIC ed indicazioni per PlasmonX* (2007), http://www.lnf.infn.it/acceleratori/plasmonx/
60. A. Giulietti, P. Tomassini, M. Galimberti, D. Giulietti, L.A. Gizzi, P. Koester, L. Labate, T. Ceccotti, P. D'Oliveira, T. Auguste, P. Monot, P. Martin, Phys. Plasmas **13**, 093103 (2006)
61. J. Meyer-ter-Vehn, A. Pukhov, Z.M. Sheng, Relativistic laser-plasma interaction, in *Proc. 30th Course of the International School of Quantum Electronics on Atoms, Solids and Plasmas in Super-Intense Laser Fields*, edited by D. Batani, C.J. Joachain, S. Martelucci, A.N. Chester (Erice, Italy, 2000), p. 167
62. A. Sharma, I. Kourakis, P.K. Shukla, Phys. Rev. E **82**, 016402 (2010)
63. A. Sharma, I. Kourakis, Laser Part. Beams **28**, 479 (2010)
64. P. Sprangle, E. Esarey, Phys. Fluids B **4**, 2241 (1992)
65. R.E. Kidder, *Interaction of intense photon and electron beams with plasmas, Physics of High Energy Density*, edited by P. Caldirola, H. Knoepfel (Academic Press, New York, 1971), p. 306
66. U. Peschel, T. Peschel, F. Lederer, J. Opt. Soc. Am. B **14**, 2994 (1997)
67. Dr. Paolo Tomassini, private communication
68. B. Qiaoa, X.T. He, S.-P. Zhu, Phys. Plasmas **13**, 053106 (2006)
69. F. Pegoraro, S.V. Bulanov, F. Califano, M. Lontano, Phys. Scr. **T63**, 262 (1996)
70. G. Askaran, S. Bulanov, F. Pegoraro, A. Pukhov, Phys. Rep. **21**, 835 (1995)
71. D. Jovanović, F. Pegoraro, F. Califano, Phys. Plasmas **8**, 3217 (2001)
72. L.M. Gorbunov, P. Mora, T.M. Antonsen, Phys. Plasmas **4**, 4358 (1997)
73. D. Jovanović, S. Vuković, Physica B+C **125**, 369 (1984)